A Novel RIS-Assisted Modulation Scheme

Liang Yang , *Member, IEEE*, Fanxu Meng , Mazen O. Hasna , *Senior Member, IEEE*,
and Ertugrul Basar , *Senior Member, IEEE*

Abstract—In this work, in order to achieve higher spectrum efficiency, we propose a reconfigurable intelligent surface (RIS)-assisted multi-user communication uplink system. Different from previous work in which the RIS only optimizes the phase of the incident users' signal, we propose the use of the RIS to create a virtual constellation diagram to transmit the data of an additional user. We focus on the two-user case and develop a tight approximation for the probability distribution function (PDF) of the minimum distance between constellation points of both users. Then, based on the proposed statistical distribution, we derive the analytical expressions of the average bit error rate of the considered two users. The letter also shows the trade off between the performance of two users as a function of the proposed phase shift at the RIS.

Index Terms—RIS, average BER, spectrum efficiency.

I. INTRODUCTION

RECONFIGURABLE intelligent surfaces (RISs) are man-made surfaces composed of electromagnetic (EM) materials, which are highly controllable by leveraging electronic devices. In essence, an RIS can deliberately control the reflection/scattering characteristics of the incident wave to enhance the signal quality at the receiver, and hence converts the propagation environment into a smart one [1].

Owing to their promising gains, recently RISs have been extensively investigated in the literature. In particular, the authors in [2] proposed a practical phase shift model for RISs. In [3], the authors studied the beamforming optimization of RIS-assisted wireless communication under the constraints of discrete phase shifts, while in [4], the authors studied the coverage and signal-to-noise ratio (SNR) gain of RIS-assisted communication systems. In [5], the authors proposed highly accurate closed-form approximations to channel distributions of two different RIS-based wireless system setups. Recently,

RISs have been used in many scenarios and have shown superior performance over systems not employing RISs. For instance, in [6], an IRS-assisted multiple-input single-output communication system is considered, and in [7], the physical layer security of RIS-assisted communication with an eavesdropping user is studied. In [8], the authors proposed RIS-assisted dual-hop unmanned aerial vehicle (UAV) communication systems while in [9], the authors used the RIS for downlink multi-user communication from a multi-antenna base station, and developed energy-efficient designs for transmit power allocation and phase shifts of the surface reflection elements. In addition, the authours considered a network assisted by multiple RISs in [10]. In [11], the authors studied the IRS-assisted spectrum sharing communication system by exploiting its passive beamforming for signal enhancement as well as interference suppression. The emerging concept of index modulation is also explored in [12] by using the RIS as a transmitter.

In all of the above studies, the advantages of RISs are mainly used to enhance the quality of the signal, and the reflection patterns were not used to carry additional information. In other words, the role of an RIS has been mainly based on the mitigation of the phase shifts of the involved channels, without any additional purpose of controlling those phase shifts. Different from the communication system based on interference cancellation in [11], in this letter, we propose a novel modulation scheme utilizing the phase shifts of the RIS in a spectrally efficient way to superimpose the data of an additional user 2 (U2) on that of the ordinary user 1 (U1).

Against this background, we consider a multi-user uplink scenario and mainly consider the feasibility of uploading the data of two users simultaneously through the RIS, where U1 sends the data to the base station through a direct link and is given a chance to utilize an available RIS-assisted link to enhance its signal, but with the condition of having the data of U2 embedded with its data through the RIS. Basically, the RIS optimizes the phase of the incident U1's signal to mitigate the phase shifts of the cascaded link as well as its direct link, and additionally to embed the data of U2 through creating a modified virtual constellation diagram. Hence, we assume that U2's data is known when the RIS optimizes the phase of the incident U1's signal, and then, a virtual constellation diagram is created by the RIS to embed U2's data. Consequently, the signal reflected by the RIS contains the data of both users. In summary, the main contributions of this work include the following: (i) we propose a novel and spectrallly efficient RIS-assisted modulation scheme, (ii) based on the proposed statistical distributions, closed-form expressions for the average bit error rates (BER) are derived and analysed.
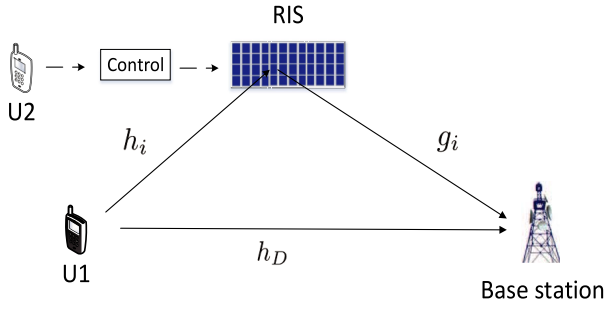
Fig. 1.   RIS-assisted uplink.

The remaining of this letter is organized as follows. Section II presents the system and channel models. The performance analysis is presented in Section III, and the numerical and simulation results are detailed in Section IV. Finally, conclusions are drawn in Section V.

II. SYSTEM AND CHANNEL MODELS

We consider the uplink system shown in Fig. 1, where U1 is communicating with the base station (BS) directly and with the help of an RIS to boost its connectivity. In the same time, U2 is in the vicinity of the RIS and is communicating with the BS through superimposing its signal on that of U1 using the RIS. It is assumed that the RIS can obtain perfect channel state information (CSI) through a control link that enables it to optimize the phase shifts of the reflected signals. As will be discussed later, the phase shifts will be utilized to super-impose U2's data on that of U1 in a way to efficiently utilize the same spectrum. This is in return of allowing U1 to take advantage of the RIS to improve its connectivity to the BS. At the receiving end, the BS first decodes the signal of U1 and extracts it from the composite received signal. In the second step, the remaining signal is processed to get the data of U2.[1]

A. Analysis of User 1

As mentioned above, U1 is communicating with the BS through the RIS-assisted dual-hop link and a direct link. An M-ary phase shift keying (MPSK) symbol x, with symbol power E_s, is sent to the RIS with N reflecting elements through a set of channels $h_i = \alpha_i e^{j\theta_i}$. Then, the RIS reflects the signal to the BS through channels $g_i = \beta_i e^{j\psi_i}$, where α_i and β_i are independent and identically distributed (i.i.d.) Rician random variables (RVs), and θ_i and ψ_i are the phases of channel gain. Meanwhile, the direct link to the BS is denoted as $h_D = \varepsilon e^{j\eta}$, where ε is a Rayleigh random variable (RV) with mean $\sqrt{\pi}/2$, variance $(4 - \pi)/4$ and η is the phase of channel gain. With the knowledge of CSI for different links (U1-RIS, RIS-BS, U1-BS), the RIS optimizes the incident signals in a way to create a virtual constellation diagram by embedding the sig-nal of U2. The overall received signal at the BS including that

---

[1]It should be noted here that users' pairing/selection and synchronization of data between users is beyond the scope of the letter and are assumed to follow standard networking schemes through different control channels.

of the direct link can be expressed as

$$
\begin{aligned}
y_1 &= \left(\sqrt{\frac{E_s}{L_1}} h_D + \sqrt{\frac{E_s}{L_2}} \sum_{i=1}^{N} h_i g_i e^{j\phi_i} \right) x + n \\
&= \left(\sqrt{\frac{E_s}{L_1}} \varepsilon + \sqrt{\frac{E_s}{L_2}} \sum_{i=1}^{N} \alpha_i \beta_i e^{jw_m} \right) e^{j\eta} x + n, \quad (1)
\end{aligned}
$$

where L_1 and L_2 are the path losses of the direct link and the RIS-assisted dual-hop link, respectively, $\phi_i = (w_m - \theta_i - \psi_i + \eta)$ is the adjustable phase introduced by the ith reflecting element of the RIS to mitigate the channels' phase shifts, w_m is the message-dependent phase introduced by the RIS to carry the information of U2 where w_m represents a binary symbol of 1 and $-w_m$ represents 0, and $n \sim \mathcal{CN}(0, N_0)$ is the additive white Gaussian noise (AWGN) signal.

Then, the received SNR at the BS can be written as

$$
\gamma_1 = \left| \sqrt{\bar{\gamma}_1} \varepsilon + \sqrt{\bar{\gamma}_2} \sum_{i=1}^{N} \alpha_i \beta_i e^{jw_m} \right|^2, \quad (2)
$$

where $\bar{\gamma}_1 = \bar{\gamma}/L_1$, $\bar{\gamma}_2 = \bar{\gamma}/L_2$ and $\bar{\gamma} = E_s/N_0$ denotes the average SNR. Then, for the considered BPSK signal, the minimum distance between constellation points is $d_1 = 2\left(\sqrt{\frac{E_s}{L_1}}\varepsilon + \sqrt{\frac{E_s}{L_2}}\sum_{i=1}^{N}\alpha_i\beta_i\cos(w_m)\right)$.

From [13, eq. (6.4)], the probability of error of BPSK modulation is given by

$$
P_b = Q\left(\frac{d_{min}}{\sqrt{2N_0}} \right), \quad (3)
$$

where $Q(\cdot)$ is the Gaussian Q-function. Thus we can get the BER of U1 as

$$
\begin{aligned}
P_{b1} &= Q\left(\frac{d_1}{\sqrt{2N_0}} \right) \\
&= Q\left(\frac{2\left(\sqrt{\frac{E_s}{L_1}}\varepsilon + \sqrt{\frac{E_s}{L_2}}\sum_{i=1}^{N}\alpha_i\beta_i cos(w_m)\right)}{\sqrt{2N_0}} \right) \\
&= Q\left(\sqrt{2R_1} \right), \quad (4)
\end{aligned}
$$

where $R_1 = (\sqrt{\bar{\gamma}_1}\varepsilon + \sqrt{\bar{\gamma}_2}\sum_{i=1}^{N}\alpha_i\beta_i\cos(w_m))^2$. From [14], we can approximate the PDF of R_1 by

$$
f_{R_1}(r) = \frac{r^{v_1-1}}{\Gamma(v_1)\lambda_1^{v_1}} e^{-\frac{r}{\lambda_1}}, \quad (5)
$$

where $v_1 = \frac{E^2(R_1)}{\text{var}(R_1)}$, $\lambda_1 = \frac{\text{var}(R_1)}{E(R_1)}$, and $\Gamma(\cdot)$ is the Gamma function [15]. Let $\chi = \sum_{i=0}^{N} \chi_i$ and $\chi_i = \alpha_i \beta_i$. Thus we have

$$
\begin{aligned}
E(R_1) &= \bar{\gamma}_1 E(\varepsilon^2) + \bar{\gamma}_2 \cos^2(w_m) E(\chi^2) \\
&\quad + 2\sqrt{\bar{\gamma}_1 \bar{\gamma}_2}\cos(w_m)E(\varepsilon)E(\chi), \quad (6) \\
\text{VAR}(R_1) &= E(R_1^2) - E^2(R_1), \quad (7)
\end{aligned}
$$

where

$$
\begin{aligned}
E(R_1^2) &= \bar{\gamma}_1^2 E(\varepsilon^4) + \bar{\gamma}_2^2 \cos^4(w_m) E(\chi^4) \\
&\quad + 4\bar{\gamma}_1^{1/2}\bar{\gamma}_2^{3/2}\cos^3(w_m)E(\varepsilon)E(\chi^3)
\end{aligned}
$$

$$+ 4\bar{\gamma}_1^{3/2}\bar{\gamma}_2^{1/2}\cos(w_m)\mathrm{E}(\varepsilon^3)\mathrm{E}(\chi)$$
$$+ 6\bar{\gamma}_1\bar{\gamma}_2\cos^2(w_m)\mathrm{E}(\varepsilon^2)\mathrm{E}(\chi^2). \qquad (8)$$

The *n*th moment of ε and χ can be calculated by

$$\mathrm{E}(\varepsilon^n) = \Gamma\left(\frac{n}{2}+1\right), \qquad (9)$$

$$\mathrm{E}(\chi^n) = \sum_{n_1=0}^{n} \sum_{n_2=0}^{n_1} \cdots \sum_{n_{N-1}=0}^{n_{N-2}} \binom{n}{n_1}\binom{n_1}{n_2}\cdots\binom{n_{N-2}}{n_{N-1}}$$
$$\times \mu_{\chi_1}(n-n_1)\mu_{\chi_2}(n_1-n_2)\cdots\mu_{\chi_N}(n_{N-1}), \qquad (10)$$

where $\mu_{\chi_i}(n) = \left(\frac{\Gamma(\frac{n}{2}+1)}{(1+K)^{\frac{n}{2}}e^K} {}_1F_1(\frac{n}{2}+1;1;K)\right)^2$ is the *n*th moment of χ_i, K is the Ricain factor, and ${}_1F_1(\cdot)$ is the Degenerate hypergeometric function [15].

B. Analysis of User 2

Assuming that the signal of U1 can be successfully decoded (represented by $\hat{x}$), the received signal can now be expressed as

$$y_2 = y_1 e^{-j\frac{2\hat{x}\pi}{M}}$$
$$= \left(\sqrt{\frac{E_s}{L_2}}\sum_{i=1}^{N}\alpha_i\beta_i e^{jw_m}x e^{-j\frac{2\hat{x}\pi}{M}} + \sqrt{\frac{E_s}{L_1}}\varepsilon x e^{-j\frac{2\hat{x}\pi}{M}}\right)e^{j\eta}$$
$$+ n e^{-j\frac{2\hat{x}\pi}{M}}$$
$$= \left(\sqrt{\frac{E_s}{L_2}}\sum_{i=1}^{N}\alpha_i\beta_i e^{jw_m} + \sqrt{\frac{E_s}{L_1}}\varepsilon\right)e^{j\eta} + n e^{-j\frac{2\hat{x}\pi}{M}}. \quad (11)$$

Looking at the constellation diagram in Fig. 2, we notice that the diagonal area represents the same information bit (i.e., upper left and lower right represent 0 for the BPSK) of U2. Our goal is to combine the same information bits and then do the decoding. Thus, the signal of U2 can be regarded as a biased BPSK signal with an initial phase of $-\frac{\pi}{M}$, and an offset angle of $\frac{\pi}{2} - w_m$. It is worth noting here that it is feasible to decode the signal directly. More specifically, we can decode the received signal as a (2*M*) PSK signal with an initial phase of $-\frac{\pi}{2M}$, so that $[0, 2, 4\cdots 2M-2]$ in the decoded data represent the 0, and $[1, 3, 5\cdots 2M-1]$ in the decoded data represent the 1 of U2. It is noted that the data obtained by the two schemes are consistent through simulation.

Then, the minimum distance between the constellation points is $d_2 = 2(\sqrt{\frac{E_s}{L_2}}\sum_{i=1}^{N}\alpha_i\beta_i\cos(\frac{\pi}{2}-w_m))$. Thus, the BER of U2 can be calculated by

$$P_{b2} = Q\left(\sqrt{2R_2}\right), \qquad (12)$$

where $R_2 = (\sqrt{\bar{\gamma}_2}\sum_{i=1}^{N}\alpha_i\beta_i\cos(\frac{\pi}{2}-w_m))^2$. Similar to the U1 case, we can get the PDF of R_2 by setting $v_2 = \frac{\mathrm{E}^2(R_2)}{\mathrm{var}(R_2)}$, $\lambda_2 = \frac{\mathrm{var}(R_2)}{\mathrm{E}(R_2)}$, where $\mathrm{E}(R_2) = \bar{\gamma}_2\cos^2(\frac{\pi}{2}-w_m)\mathrm{E}(\chi^2)$ and $\mathrm{var}(R_2) = \bar{\gamma}_2^2\cos^4(\frac{\pi}{2}-w_m)(\mathrm{E}(\chi^4)-\mathrm{E}^2(\chi^2))$.

III. PERFORMANCE ANALYSIS

In this section, we analyze the performance of the proposed scheme by deriving closed-form expressions for the average

BER. For BPSK modulation schemes, a unified average BER expression is given by [16, eq. (12)]

$$P_e = \int_0^{\infty} Q\left(\sqrt{2\gamma}\right)f_\gamma(\gamma)d\gamma$$
$$= \frac{1}{2\Gamma(\frac{1}{2})}\int_0^{\infty}\exp(-\gamma)\gamma^{-\frac{1}{2}}F_\gamma(\gamma)d\gamma, \qquad (13)$$

where $F_\gamma(\gamma)$ is the cumulative distribution function (CDF) of $\gamma \in \{R_1, R_2\}$.

1) *Average BER of User 1:* From [15, eq. (3.381)], [17, eq. (07.34.21.0088.01)] and (5), P_{e1} can be formulated as

$$P_{e1} = \frac{1}{2\Gamma(\frac{1}{2})\Gamma(v_1)}\mathrm{G}_{2,2}^{1,2}\left(\frac{1}{\lambda_1}\Big|\begin{matrix}\frac{1}{2},1\\v_1,0\end{matrix}\right), \qquad (14)$$

where $\mathrm{G}_{2,2}^{1,2}(\cdot)$ is the Meijer-G function [15]. Asymptotically, when $\bar{\gamma} \to \infty$, and with the help of [17, eq. (07.34.06.0006.01)], we have

$$P_{e1} \to \frac{\Gamma\left(v_1 + \frac{1}{2}\right)}{\Gamma(\frac{1}{2})\Gamma(v_1+1)\lambda_1^{v_1}}. \qquad (15)$$

2) *Average BER of User 2:* As the decoding of U2 signal follows that of U1, it is usually difficult to ensure that the decoded signal is completely correct. Therefore, after processing the received signal, we might get some inverted information bits of U2. Then, the practical average BER of U2 can be expressed as

$$P_{e2} = P_{e2}^{ideal}(1 - P_{e1}) + P_{e1}(1 - P_{e2}^{ideal}), \qquad (16)$$

where P_{e2}^{ideal} denotes U2's average BER with ideal conditions (i.e., assuming the decoded U1's data is completely correct). From (12) and (13), and using [15, eq. (6.455)], the ideal U2's average BER can be calculated as

$$P_{e2}^{ideal} = \frac{1}{2\Gamma(\frac{1}{2})\Gamma(v_2)}\mathrm{G}_{2,2}^{1,2}\left(\frac{1}{\lambda_2}\Big|\begin{matrix}\frac{1}{2},1\\v_2,0\end{matrix}\right), \qquad (17)$$

and when $\bar{\gamma} \to \infty$, we have

$$P_{e2}^{ideal} \to \frac{\Gamma\left(v_2 + \frac{1}{2}\right)}{\Gamma(\frac{1}{2})\Gamma(v_2+1)\lambda_2^{v_2}}. \qquad (18)$$

Thus the asymptotic expression of U2 can be calculated as $P_{e2} \to P_{e1} + P_{e2}^{ideal}$.

IV. NUMERICAL AND SIMULATION RESULTS

In this section, we present some numerical results to verify our analysis. The parameters used in the figures are $K = 3$, $L_1 = 30$ dB, and $L_2 = 40$ dB.

In Fig. 2 we plot the constellation diagram of U1 and U2 where $\bar{\gamma} = 0$ dB, and $w_m = \pi/4$. It can be deduced from Fig. 2 that superimposing U2's data on that of U1 causes the constellation diagram of U1's to shift based on the value of w_m used. This causes the BER of U1 to increase, simply because the separation of the two constellation points is lower at this time. From the constellation of U2, it can be deduced that the processed signal is similar to a BPSK signal where the initial phase is $-\pi/2$.

In Fig. 3, we plot the average BER of U1 as a function of w_m. When $w_m = 0$, this is equivalent to the case where there
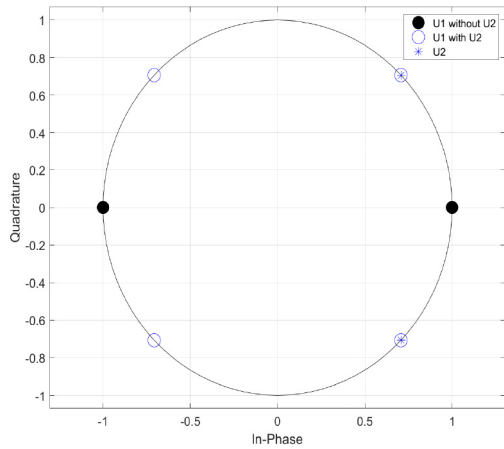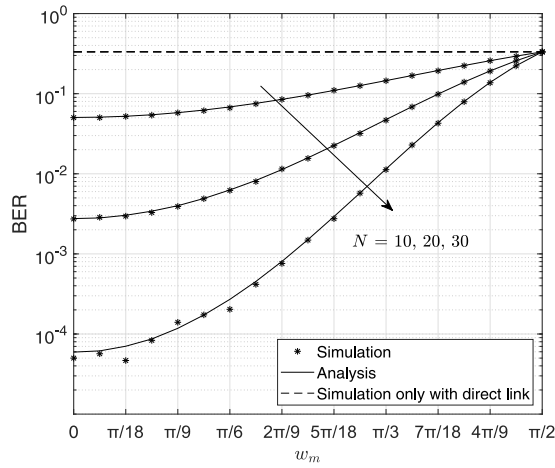
Fig. 2. The constellation diagram of U1 and U2.

Fig. 3. Average BER of U1 versus w_m.

Fig. 4. Average BER of U2 versus w_m.

Fig. 5. Average BER of U1 versus $\bar{\gamma}$ with and without U2.

is no U2 and only the data of U1 is transmitted in the uplink, and its constellation is a pure BPSK one. As we increase w_m, the system needs to utilize the spectrum resources of U1 to transmit the signal of U2. Consequently, U1's average BER increases. When w_m reaches $\pi/2$, it leads to the lowest data accuracy of U1. In addition, and as expected, it can be seen from Fig. 3 that increasing N can bring performance improvements to U1. This means that we can reduce the negative effect of w_m by increasing N.

In Fig. 4, we plot the average BER of U2 versus w_m. It is clear from the figure that by increasing w_m, the average BER of U2 decreases first and then increases. When w_m is small, P_{e1} is small, and hence the system performance is mainly determined by P_{e2}^{ideal}. Similar to the observations in Fig. 3, increasing w_m causes P_{e1} to increase, and when w_m is large, one cannot get a clean U2 signal due to the large average BER of U1. Hence, the system performance is dominated in this case by P_{e1}. This means that the choice of w_m is critical to ensure reasonable performance of both users.

In Fig. 5, we plot the average BER of U1 versus $\bar{\gamma}$ with and without U2. As expected, increasing the average SNR leads to decreasing the average BER. In addition, the effect of having U2 on the average BER of U1 is clear from the
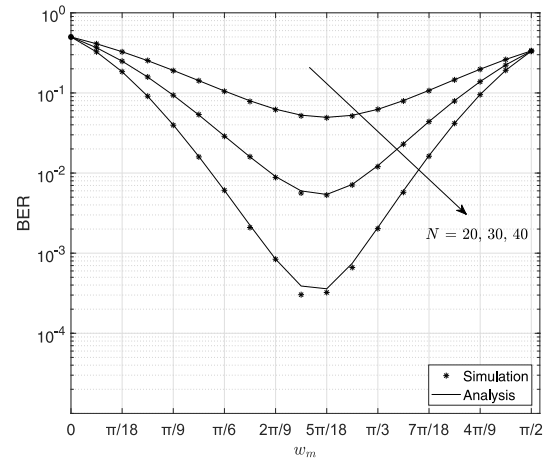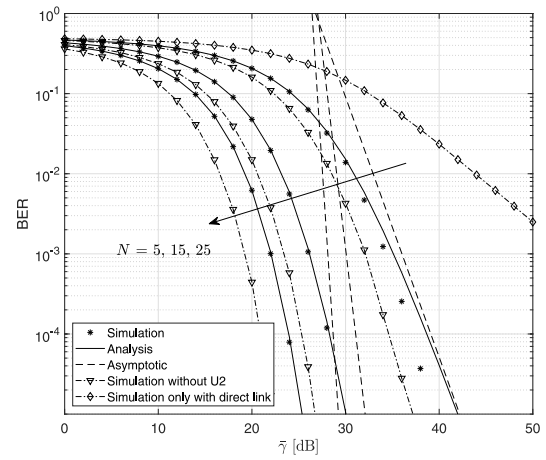
figure. The figure shows also the performance of U1 when using the direct link only. It is clear that the incentive given to U1 through the RIS usage to allow the superposition of U2 data is worthy to U1 from performance point of view. Finally, we observe a close match between the derived expressions and the simulation results which confirms the accuracy of the analytical expressions.

In Fig. 6, we plot the BER of U2 versus $\bar{\gamma}$ with $w_m = -\frac{\pi}{4}$, where Fig. 6 (a) represents the practical conditions and Fig. 6 (b) represents the ideal conditions. Similar to the observations in Fig. 5, increasing $\bar{\gamma}$ and N, causes the BER to decrease. From Fig. 6(a), increasing the SNR and/or the number of elements N, reduces the impact of the direct link on the BER performance of the system. Simultaneously, it can be found from Fig. 6(b) that the existence of the direct link has no effect on the BER performance of U2 under ideal conditions. The fundamental reason is that the direct link has no effect on the minimum distance between constellation points of U2s' different information bits. In actual situations, the direct link causes the BER of U2 to decrease. This can be explained by the fact that the existence of a direct connection reduces the BER of U1, which decreases the BER of U2.
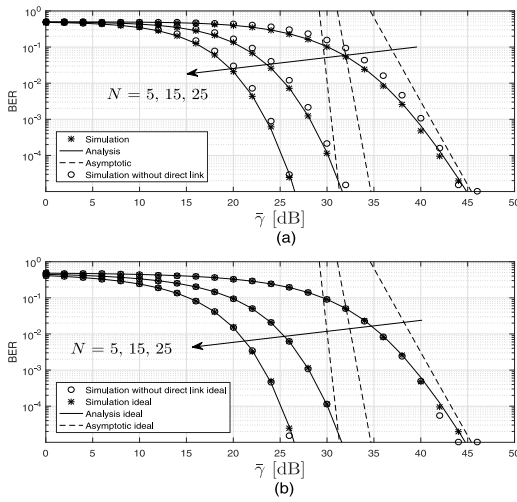
Fig. 6. Average BER of U2 versus $\bar{\gamma}$ (a) practical and (b) ideal conditions.
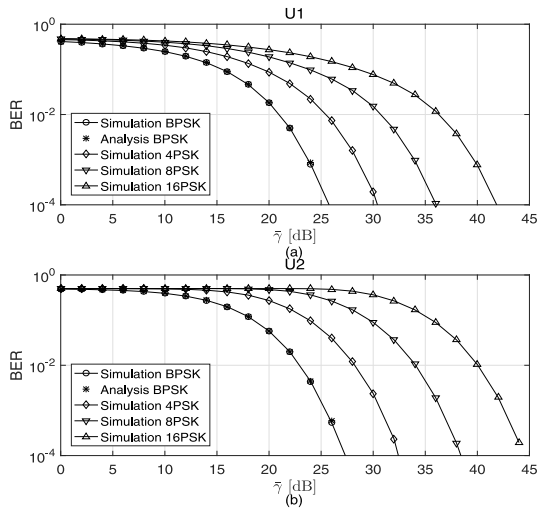

Fig. 7. Average BER versus $\bar{\gamma}$ with different modulation.

In Fig. 7, we plot the BER of U1 and U2 versus $\bar{\gamma}$ with different modulation orders where $w_m = \frac{\pi}{2M}$ and $N = 20$. From Fig. 7, we can notice that the use of higher order modulation levels leads to an increase in the BER of the two users, as expected. The main reason is that higher order modulation levels lead to a decrease in the Euclidean distance between the constellation points.

V. Conclusion

In this letter, we have proposed an RIS-assisted multi-user uplink communication system employing a novel modulation scheme. More specifically, we have derived an analytical expression of the average BER and a tight approximation on the PDF of the minimum distance between constellation points of the case of two users sharing the same spectrum with the help of an RIS. Numerical results show that we can obtain U2's data with higher accuracy while ensuring the accuracy of U1's data by setting an appropriate phase shift and large enough number of surface elements. In future work, we will take the imperfect CSI and hardware impairments into consideration and investigate their effects on our proposed scheme. Furthermore, we will extend our analysis to the multiuser scenario.

References

[1] E. Basar, M. D. Renzo, J. de Rosny, M. Debbah, M.-S. Alouini, and R. Zhang, "Wireless communications through reconfigurable intelligent surfaces," *IEEE Access*, vol. 7, pp. 116753–116773, 2019.

[2] S. Abeywickrama, R. Zhang, Q. Wu, and C. Yuen, "Intelligent reflecting surface: Practical phase shift model and beamforming optimization," *IEEE Trans. Commun.*, vol. 68, no. 9, pp. 5849–5863, Sep. 2020.

[3] Q. Wu and R. Zhang, "Beamforming optimization for wireless network aided by intelligent reflecting surface with discrete phase shifts," *IEEE Trans. Commun.*, vol. 68, no. 3, pp. 1838–1851, Mar. 2020.

[4] L. Yang, Y. Yang, M. O. Hasna, and M.-S. Alouini, "Coverage, probability of SNR gain, and DOR analysis of RIS-aided communication systems," *IEEE Wireless Commun. Lett.*, vol. 9, no. 8, pp. 1268–1272, Aug. 2020.

[5] L. Yang, F. Meng, Q. Wu, D. B. da Costa, and M.-S. Alouini, "Accurate closed-form approximations to channel distributions of RIS-aided wireless systems," *IEEE Wireless Commun. Lett.*, vol. 9, no. 11, pp. 1985–1989, Nov. 2020.

[6] X. Hu, J. Wang, and C. Zhong, "Statistical CSI based design for intelligent reflecting surface assisted MISO systems," *Sci. China Inf. Sci.*, vol. 63, Oct. 2020, Art. no. 222303, doi: 10.1007/s11432-020-3033-3.

[7] L. Yang, J. Yang, W. Xie, M. Hasna, T. Tsiftsis, and M. D. Renzo, "Secrecy performance analysis of RIS-aided wireless communication systems," *IEEE Trans. Veh. Technol.*, vol. 69, no. 10, pp. 12296–12300, Oct. 2020.

[8] L. Yang, F. Meng, J. Zhang, M. O. Hasna, and M. D. Renzo, "On the performance of RIS-assisted dual-hop UAV communication systems," *IEEE Trans. Veh. Technol.*, vol. 69, no. 9, pp. 10385–10390, Sep. 2020.

[9] C. Huang, A. Zappone, G. C. Alexandropoulos, M. Debbah, and C. Yuen, "Reconfigurable intelligent surfaces for energy efficiency in wireless communication," *IEEE Trans. Wireless Commun.*, vol. 18, no. 8, pp. 4157–4170, Aug. 2019.

[10] L. Yang, Y. Yang, D. B. da Costa, and I. Trigui, "Outage probability and capacity scaling law of multiple RIS-aided networks," *IEEE Wireless Commun. Lett.*, vol. 10, no. 2, pp. 256–260, Feb. 2021.

[11] X. Guan, Q. Wu, and R. Zhang, "Joint power control and passive beamforming in IRS-assisted spectrum sharing," *IEEE Commun. Lett.*, vol. 24, no. 7, pp. 1553–1557, Jul. 2020.

[12] E. Basar, "Reconfigurable intelligent surface-based index modulation: A new beyond MIMO paradigm for 6G," *IEEE Trans. Commun.*, vol. 68, no. 5, pp. 3187–3196, May 2020.

[13] A. Goldsmith, *Wireless Communications*. Cambridge, U.K.: Cambridge Univ. Press, 2005.

[14] D. B. C. Battikh, J. M. Kelif, M. Coupechoux, and P. Godlewski, "SIR distribution analysis in cellular networks considering the joint impact of path-loss, shadowing and fast fading," *EURASIP J. Wireless Commun. Netw.*, vol. 2011, no. 4, pp. 1064–1071, 2011.

[15] I. S. Gradshteyn and I. M. Ryzhik, *Table of Integrals, Series, and Products*, 7th ed. San Diego, CA, USA: Academic, 2007.

[16] I. S. Ansari, S. Al-Ahmadi, F. Yilmaz, M.-S. Alouini, and H. Yanikomeroglu, "A new formula for the BER of binary modulations with dual-branch selection over generalized-K composite fading channels," *IEEE Trans. Commun.*, vol. 59, no. 10, pp. 2654–2658, Oct. 2011.

[17] *The Wolfram Functions Site*, WOLFRAM, Champaign, IL, USA, 2001. [Online]. Available: http://functions.wolfram.com